Coastal Dynamics 2017
Paper No. 267

TIDAL ENERGY DISSIPATION IN THREE ESTUARINE ENVIRONMENTS

Salme Cook[1] and Tom Lippmann[1]

Abstract

Tidal energy dissipation was examined in three estuaries using a three-dimensional hydrodynamic model (COAWST; Warner, et al., 2010). The modeled M2 tidal amplitude decay and phase lag were estimated at specific locations along transects from the mouths of the estuaries to the furthest inland extent, and compared to observations where available. Nonlinear evolution of the tides was qualitatively examined with the spatial evolution of the skewness and asymmetry, and the growth of harmonic constituents. Harmonic constituents and over-tides were estimated from modeled time series of water levels and three-dimensional currents with T_TIDE (Pawlowicz, 2002). Observed evolution of tidal dissipation, harmonic growth, and nonlinear statistics are also well modeled, indicating that the nonlinear evolution of the tides is well represented in COAWST.

Key words: estuarine hydrodynamics, tidal asymmetry, numerical modeling

1. Introduction

Astronomical tides are the dominant force in most coastal and estuarine environments, driving the transport of water, sediment, nutrients, and organisms between terrestrial and marine ecosystems. As tides propagate across the ocean and into shallow inlets and bays, they interact with the bottom and become distorted, leading to asymmetries in the duration of the tide and magnitude of the tidal currents, and growth of the tidal harmonics. The asymmetries arise from the inherently nonlinear nature of the tidal shoaling process, leading to the development of local phase lags between pressure and velocities that shift slack tide periods up to 90 degrees (or ¼ wave period). When averaged over a tidal cycle this asymmetrical behavior determines net sediment transport and circulation patterns (Dronkers, 1986). This behavior has important implications for sediment transport where stronger flood currents drive the movement of coarse sediment and longer slack periods lend themselves to the deposition of fine-grained sediment.

Tidal propagation also leads to amplitude attenuation from energy losses due to frictional interaction with the bottom and geometry of the estuary. Energy dissipation of the tidal wave can be described in terms of amplitude decay of the dominant tidal constituent; the semi-diurnal M_2 tide in this study. Not all energy is dissipated due to frictional effects, and some is transferred to higher harmonics (overtides, e.g. M_4 and M_6) through nonlinear interactions that create tidal asymmetry (Aubrey and Speer, 1985, Speer and Aubrey, 1985). A comparison of the magnitude and phase differences of the M_2 with the first harmonic M_4 qualitatively describes the tidal asymmetries in the system (Friedrichs and Aubrey, 1988).

In this work, we model the tidal motion in three distinct estuaries with a three-dimensional, high resolution hydrodynamic model and examine the nonlinear evolution as the tides propagate upstream. The model used is the Coupled Ocean-Atmosphere-Wave-Sediment Transport modeling system (COAWST; Warner, *et al*., 2008). COAWST includes state-of-the-art atmospheric (WRF) and wave (SWAN) models coupled with the Regional Ocean Modeling System (ROMS;), a three-dimensional fully nonlinear hydrodynamic, ortho-curvilinear primitive equation model (Shchepetkin and McWilliams, 2005; Haidvogel *et al*. 2008). Previous hydrodynamic modeling and observational studies of tidal inlets show that nonlinear advection, nonlinear channel friction and tidal interaction with coastal geometry drive tidal distortion (Dronkers, 1986, Aubrey and Speer, 1985, Speer and Aubrey, 1985), and that evolution of the tides is strongly

[1]Department of Earth Sciences, University of New Hampshire, 56 College Road, 214 James Hall, Durham, New Hampshire, United States of America. sc10@wildcats.unh.edu

dependent on the bottom boundary conditions (*e.g.*, MacMahan, et al., 2014).

We will examine the nonlinear tidal behavior that drive tidal asymmetry and energy decay in each estuary, and discuss modeled tidal dissipation characteristics in terms of tidal amplitude decay and phase lags determined from harmonic analysis of tidal constituents. Modeled results are compared with observations where available or with previous results from the literature. Section 2 provides site background and model grid development of each estuary, Section 3 describes the model and tidal analysis methodology, Section 4 discusses the results in terms of nonlinear evolution, and Section 5 summarizes the conclusions of the study.

2. Site background and model grid development

Each of the three estuaries in this study are well mixed and tidally driven, and river influences are considered negligible. New River Inlet, NC (Figure 1A; discussed in Section 2.1) demonstrates progressive wave characteristics and a highly dissipative environment. Hampton Inlet, NH (Figure 1B; discussed in Section 2.2) demonstrates very different dynamics than New River Inlet, as the tide acts like a standing wave as it propagates inshore on two branches of the estuary, and like a progressive wave on the third. The Piscataqua River-Great Bay system, NH (Figure 1C; discussed in Section 2.3) is characterized by both progressive and standing wave characteristics, depending upon the section of the main branch of the estuary. In order to characterize the tidal wave properties, time series were extracted from stations within each estuary (Figure 1).

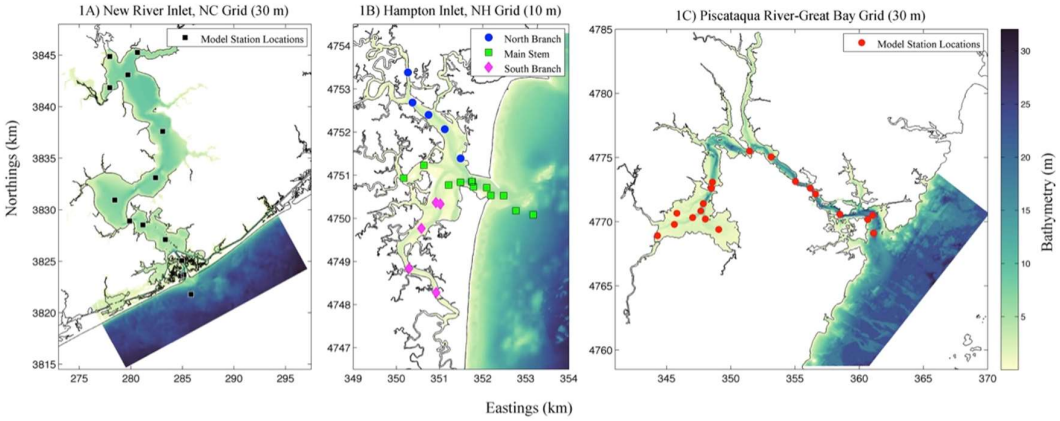

Figure 1: Model Grid Bathymetry and Station Locations, 1A) New River Inlet, North Carolina, 1B) Hampton Inlet, New Hampshire, and 1C) Piscataqua River-Great Bay estuary, New Hampshire.

2.1. *New River Inlet, North Carolina*

New River Inlet is a part of the White Oak River Basin located in the Carolina Cape region of North Carolina. It serves as an important habitat for birds and fish, an economic resource for commercial fisherman, as well as a strategic location for the Camp Lejeune Marine Corps military base. The New River estuary is a coastal plain system, influenced by barrier islands and the Atlantic Intracoastal Waterway. For decades the inlet has been dredged in order to maintain a navigable channel. The inlet is 1 km wide at the mouth, and has a mean tide range of 1.31 m. Water depths range from 1-3 m at the mouth, over 10 m in the main channel, and again ranging 1-3 meters over an extensive estuarine back bay. The watershed drains an area of 1197 km^2, and has a surface area of 88 km^2 (NOAA, 1999). Historically it has been described as eutrophic, with excessive nutrient loading from local wastewater treatment facilities and historical hog waste dumping,(Burkholder *et al.* 1997; Mallin *et al*. 1997). Despite recent improvements in both treatment facilities and non-point source loading, eutrophication still persists because New River is a shallow and poorly flushed system.

Observations show that the principal semi-diurnal amplitude decays by about 87% from the mouth to 10 km upstream, consistent with a strongly tidally-choked system (MacMahan, et al., 2014). A simple model balancing the pressure gradient by a quadratic bottom friction formulation suggests that nonlinear interactions induced by the bottom drag modify the amplitude and phase changes of the tide as it propagates upstream.

2.1.1. *New River Inlet: Model Grid*
For the implementation of COAWST at New River Inlet, we generated a structured orthonormal grid with constant 30 m horizontal resolution and 8 vertical sigma levels. The bathymetric dataset used for this grid was created using a 10-m digital elevation model (DEM) that includes several sources of topography (Lidar) and bathymetry(hydrographic surveys), interpolated using Fledermaus software, and compiled by the researchers at the United States Army Corps of Engineers (USACE) Field Research Facility (FRF).

2.1.2. *New River Inlet: Model Setup*
The model is forced with five tidal constituents (M2, N2, S2, O1, K1). The harmonic constituents were obtained using values from Wrightsville Beach, NC, harmonic station (#8658163), from the NOAA Tide Prediction service (http://tidesandcurrents.noaa.gov), and shown in Table 1. Tides were forced on the open boundary at the ocean about 2 km from shore. The lateral boundaries within the inlet at the junctions with the Atlantic Intracoastal Waterway (ICW) were left open. For the purposes of this study, no mean flow was forced through the ICW, nor was any river discharge (typically small) from any tributary flowing into the inlet considered. A total of 14 model stations were placed from the open ocean to the head of the estuary, near the town of Jacksonville, NC (Figure 1A).

2.2. *Hampton Inlet, New Hampshire*

The Taylor River, and Hampton Falls River feed Hampton River to the north and Blackwater River to the south that drain through Hampton Inlet, a barrier beach system located in southeastern New Hampshire in the Gulf of Maine. With direct and easy access to the Atlantic Ocean, the harbor is home to several commercial fishing and recreation charter boating businesses. The inlet is maintained through regular dredging conducted by the United States Army Corps of Engineers (USACE) and is stabilized by two jetties on either side of the inlet. Hampton Beach is located directly north of the inlet and through predominantly southern alongshore transport, sedimentation builds shoals on the north side of the inlet and form a spit to the south. Tidal currents on flood and ebb tides can exceed 2 meters per second respectively (Mckenna, 2013). Strong currents and active shoaling lead to potentially hazardous navigational conditions. Extensive salt marshes characterize the backbay with several flats used for recreational shellfishing.

2.2.1. *Hampton Inlet: Model Grid*
The horizontal grid used at Hampton Inlet was similar to New River, with horizontal resolution of 30 m, with 8 vertical sigma levels. The bathymetric grid is compiled from seven different Lidar and hydrographic sources, ranging in years from 1999 to 2015 and acquired from NOAA's coast dataviewer database and the Western Gulf of Maine (WGOM) dataset compiled at the Center for Coastal and Ocean Mapping-Joint Hydrographic Survey (CCOM/JHC) at the University of New Hampshire.

2.2.2. *Hampton Inlet: Model Setup*
The model again is forced with five tidal constituents (M2, N2, S2, O1, K1) at the offshore open boundary. The harmonic constituents were obtained using Oregon State University's global Tidal Prediction Software Package (OTPS) in conjunction with the United States East Coast Regional Tidal Solution (EC2010) (Egbert, 2002). This software package provided the necessary tidal amplitude and phases (shown in Table 1) that correspond to 19 September 2011, thereby coinciding with some of the observational datasets for future model-data comparisons. A total of 21 model stations were placed from the open ocean to the head of each branch of the estuary (North, Middle, and South; Figure 1B).

2.3. *Piscataqua-River Great Bay Estuary, New Hampshire*

The Great Bay/Piscataqua River estuarine system is located along the New Hampshire-Maine border. The Little Bay-Great Bay estuary is a recessed, drowned river valley connected to the Gulf of Maine via the Piscataqua River. There are seven major tributaries in this system, including the Squamscott, Lamprey, Oyster, Bellamy, Cocheco, Salmon Falls, and Winnicut rivers. Tidal excursion up these rivers is blocked by dams, which regulate the freshwater input into the system. Overall, the freshwater input is relatively small and only 2% of the tidal prism (Short, 1992; Trowbridge, 2007). The tide range is 2-4 m over the spring-neap cycle with tidal currents exceeding 2 m/s in the channels at maximum ebb and flood tides. At low stands of the tide as much as 50% of the Great Bay is exposed as low-lying mudflats, incised by deeper tidal channels.

2.3.1. *Piscataqua-River Great Bay estuary: Model Grid*

Again, the horizontal grid resolution is 30 m, with 8 vertical sigma levels. Bathymetric data from several sources (CCOM/JHC, USGS, NOAA, and USACE) were compiled, weighted based on coverage and resolution, and then interpolated to create a composite DEM. The combined elevation data were used with the Easygrid routine to create the model grid (available at https://www.myroms.org/wiki/easygrid). Unlike the other two case studies, this grid required extensive smoothing in areas with steep bathymetry gradients in order to obtain numerical stability.

2.3.2. *Piscataqua-River Great Bay estuary: Model Setup*

The model is forced with five tidal constituents (M2, N2, S2, O1, K1) at the open boundary offshore. The amplitudes and phases for these constituents were obtained through harmonic analysis using T_TIDE (Paw lowicz, 2002) and a surface elevation dataset from 28 March 2006 as a part of the NOAA Marine Aquaculture Program. The amplitudes and phases are presented in Table 1. A total of 21 model stations (save points) were placed from the open ocean to the head of the estuary (Figure 1C).

2.3.3. *Piscataqua-River Great Bay estuary: Observations*

Field observations of horizontal currents spanning the water column, sea surface elevation (from bottom pressure and tide gauge), water temperature, and salinity were obtained during field experiments in 2007 and 2015, the long term Great Bay Buoy (http://www.opal.sr.unh.edu/data/buoys/great_bay), and the NOAA Tide Gauge station at Fort Point, NH (Station ID 8423898). Between May and September 2007 bottom-mounted, upward-looking acoustic Doppler current profilers (ADCPs) were deployed in the tidal channel from the mouth of the Piscataqua River to Furber Strait within the Great Bay in water depths ranging between 4.3 m and 19.3 m. A total of 11 different deployments collected current, temperature, and conductivity data for record lengths between 41-45 days (data available at https://tidesandcurrents.noaa.gov). Between August and September 2015 four ADCPs were used in 8 different deployments in Great Bay proper, in water depths ranging between 3 m on the mudflats and 17 meters in the main channel. Currents measurements were sampled continuously, for record lengths between 8-35 days.

Table 1. Tidal harmonic amplitudes and phases for each model case. The top number is the amplitude in meters (m), while the bottom number is in degrees, referenced to GMT.

Model Case	Tidal Harmonic Constituent				
	Semi-diurnal			Diurnal	
	M2	N2	S2	O1	K1
New River, NC	0.593 (m) 351.3	0.142 (m) 333.7	0.103 (m) 14.1	0.069 (m) 192.6	0.096 (m) 186.4
Hampton Inlet, NH	1.310 (m) 254.6	0.296 (m) 98.04	0.210 (m) 139.8	0.100 (m) 256.1	0.134 (m) 279.1
Piscataqua River – Great Bay, NH	1.328 (m) 300.3	0.248 (m) 274.8	0.179 (m) 179.2	0.113 (m) 107.8	0.145 (m) 126.5

3. Methods

3.1 Hydrodynamic Model

The hydrodynamic model used is the Regional Ocean Modeling System (ROMS) within the Coupled Ocean Atmosphere Wave and Sediment Transport (COAWST) modeling system. ROMS is a three-dimensional finite difference model that solves the Reynolds-averaged Navier-Stokes equations using the hydrostatic and Boussinesq assumptions (Shchepetkin and McWilliams, 2005). Measured bathymetric data were used to define the model grid (discussed in Section 2). The tidal forcing (Table 1) are ramped up hyperbolically over a 2-day period. The bottom boundary conditions are based on a logarithmic drag law, derived from a characteristic bottom roughness element. A k-ε generic length scale (GLS) turbulence closure model is used to calculate the horizontal and vertical eddy viscosities (Umlauf and Burchard, 2003; Warner et. al., 2005). Each model is run for 30 days with output of averaged data over the whole domain at 30-minute intervals and at specific station locations at 5-minute intervals. Within ROMS the wetting and drying algorithm (Warner, et. al., 2013) is utilized to simulate the inundation and exposure of the mudflats by the tide in shallow areas. The critical depth, D_{crit} is set to 10 cm; when the total water depth is less than D_{crit}, no flux is allowed in or out of that cell and it is considered "dry". Model parameters are shown in Table 2.

Table 2. Model Parameters.

Model Case	Model Parameter			
	Grid Size	Horizontal Resolution	Vertical Resolution	Bottom Roughness
New River, NC	399 x 599	30 meters	8 sigma layers	0.015
Hampton Inlet, NH	526 x 784	10 meters	8 sigma layers	0.02
Piscataqua River – Great Bay, NH	734 x 834	30 meters	8 sigma layers	0.015

3.2 Tidal Dissipation Analysis

As the tide propagates into inlets, bays, and other coastal regions, it interacts with the bottom boundary and basin geometry, and loses energy in the form of small turbulent motions. Energy dissipation results in tidal amplitude decay and phase changes that modifies the asymmetries of the waveform and flow field. Figure 2 shows modeled time series for the sea surface elevation change in the Piscataqua River-Great Bay model case from. There is a noticeable change between the station closest to the ocean (Fort Point, NH – mouth of the Piscataqua River) to the back-bay area of the Great Bay proper near the Squamscott railroad bridge. Results for New River and Hampton are discussed in Section 4.

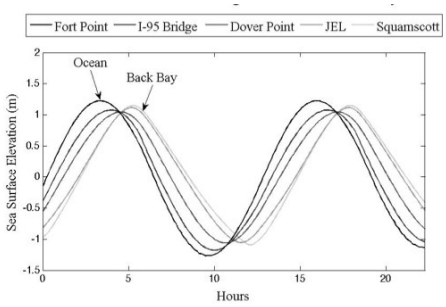

Figure 2: Modeled time series of the tidal amplitude decay for the Piscataqua River-Great Bay model case.

The total energy per unit surface area of any tidal constituent is,

$$E = 1/2\,\rho g A^2 \quad (1)$$

where ρ is the density of water, g is the acceleration due to gravity, and A is the amplitude of that constituent (dominated by the M_2 tide in our estuaries). The amplitude at any location within the estuary,

$A_{station}$, can be normalized by the ocean amplitude, A_{ocean}, and squared to represent the fractional energy loss, E, as the tide propagates inland,

$$E_{norm}=(A_{station}/A_{ocean})^2 \quad (2)$$

The normalized energy decay of the M_2 tide is shown in Figure 3 and demonstrates that about 40% of the M2 tidal signal is dissipated through the narrow, high flow Piscataqua River at a distance about 12 km into he estuary near the entrance to the Little Bay. Further inland over the next 13 km very little energy is lost. Coincident with the energy decay is a nearly linear change in phase to about 45 degrees at the 12 km point, and then nearly constant phase within the Great Bay beyond 18 km in the expansive and relatively shallow Great Bay region with extensive mud flats.

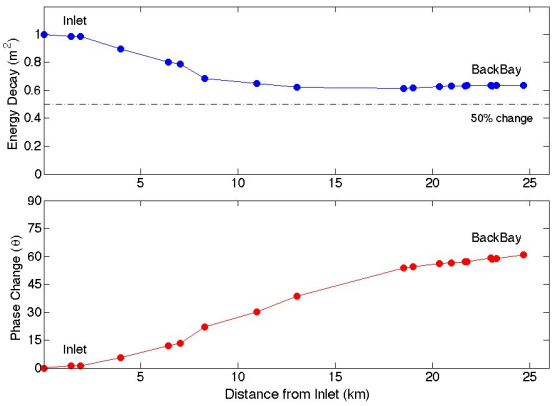

Figure 3: Normalized energy decay and phase change of the M_2 tidal constituent as a function of distance from the ocean (inlet) for the Piscataqua River-Great Bay model case.

A comparison of this phase change to the higher harmonics, M_4 and M_6, is an indication of the flood or ebb dominance and asymmetry in the system (see Section 3.4).

The corresponding results for New River Inlet, NC and Hampton Inlet, NH are shown in Figure 6 and discussed in Section 4.

3.3 Time Series Analysis

Time series of sea surface height and depth averaged currents in the u (east-west) and v (north-south) directions were retained at each station. Velocities were rotated to align with the along-channel direction using standard rotary analysis. Figure 4 shows a time series of sea surface height (red line), and the along-channel velocity component (black line), for five locations in the Piscataqua River-Great Bay estuary. In the top panel, the velocity lags the elevation time series by approximately 50 degrees, indicating a mix of shoreward progressive and seaward-reflected wave components. The middle panels indicate a shift in phase differences from velocity leading to velocity lagging in the vicinity of entrance to the Little Bay (at the General Sullivan Bridge). The bottom panel, from the upstream extent of the Great Bay near the Squamscott railroad bridge, shows an asymmetric, pitched forward sea surface height profile that leads the upstream directed velocity maxima by almost 90 degrees, consistent with a standing tidal waveform. Estimates of the phase difference between sea surface height and along-channel velocities are shown by the cross spectra in Figure 5 for the station nearest the ocean boundary and the most upstream station.

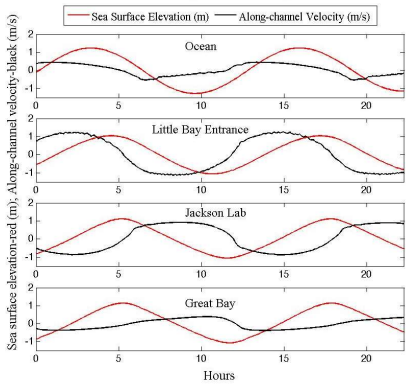

Figure 4: Sea surface elevation and along-channel velocity time series from the Piscataqua River-Great Bay model case. Top panel is from the station closest to the ocean, and each subsequent panel is closer to the back bay.

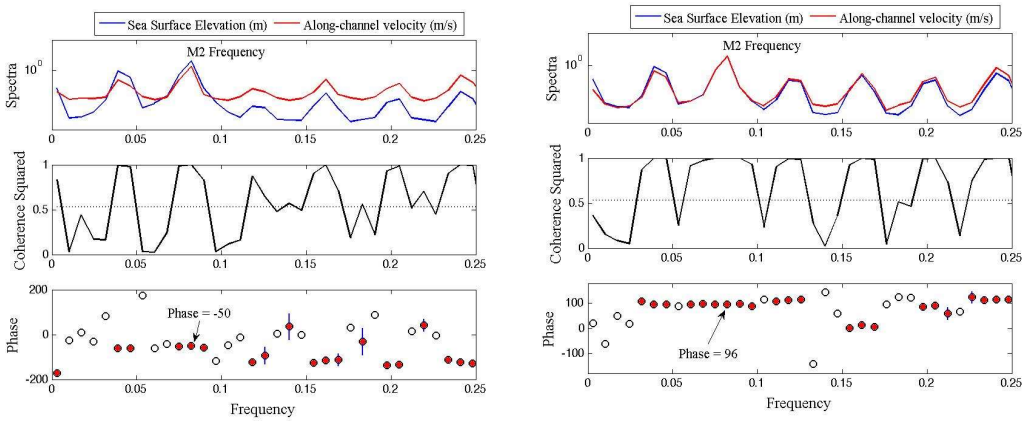

Figure 5: Spectral analysis of the Ocean station [Left] and Great Bay station [Right]. Top panel is the spectra of the sea surface elevation (blue) and the along-channel velocity (red), coherence squared, and phase. Significant phases are filled and include confidence intervals and for most of the significant phases the confidence intervals are smaller than the marker size. For the M2 frequency, the phase at the ocean station is about 50 degrees out of phase, and 96 degrees out of phase at the Great Bay station location. Spectra were computed with a Hanning data window and 10 degrees-of-freedom.

*3.4 **Nonlinear Harmonic Growth***

The growth of the M_4 harmonic relative to the M_2 constituent is a measure of the asymmetry and non-linear distortion of the tide (Friedrichs and Aubrey, 1988). Spectra of sea surface elevation time series from three stations spanning the estuary show the growth of the M_4 and M_6 harmonics (in particular) as the tide shoals upstream (Figure 5). Following Speer and Aubrey (1985), the amplitude ratio and the phase difference defined as,

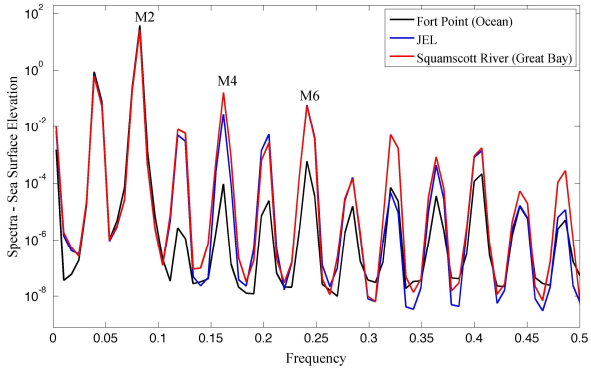

Figure 5: Spectral analysis of three stations show the growth of the M4 and M6 higher harmonics from the ocean to the bay. Spectra were computed with a Hanning data window and 10 degrees-of-freedom.

$$A_{diff}=A_{M4}/A_{M2} \quad (3)$$

$$\theta_{diff}=2*\theta_{M2}-\theta_{M4} \quad (4)$$

where A_{M4} and A_{M2} are the amplitudes of the M_4 and M_2 sea surface elevation or velocity, respectively, and θ_{M4} and θ_{M2} represent corresponding phase relationships between the constituents. In general stronger frictional effects produce larger M_4/M_2 ratios and the phase differences describe flood or ebb dominance. Phase differences between 0° and 180° indicate flood-dominance, and between 180° and 360° ebb dominance. Flood dominant systems have characteristically longer falling than rising tides, and ebb dominant systems have characteristically longer rising tides. Harmonic analysis of the station data provides the phases and amplitudes for these components (discussed in Section 4).

4. Discussion

4.1 Tidal Dissipation

Energy decay of the M_2 tidal constituent relative to the value at the entrance is shown in Figure 6 as a function of distance from the mouth of each respective estuary. Each region has markedly different dissipation characteristics, with the 92% and 40% energy loss at New River and Great Bay, respectively, whereas energy variation in Hampton shows very little dissipation in the north and middle branches, but 80% loss in the south channel.

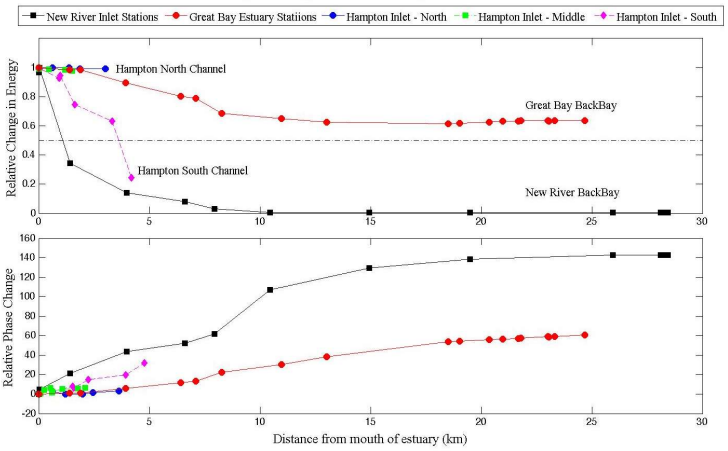

Figure 6: Relative energy decay and phase change in the M2 tidal signal for all of the model cases.

Relative phase change as a function of distance up the estuary shown in Figure 6, corresponds to the relative dissipation differences in each estuary. New River Inlet shows the greatest phase change (~145) whereas Hampton Inlet shows the lowest (<10). New River Inlet acts as a progressive wave, with a sea surface elevation-along-channel velocity phase closer to 0˚ than 90˚ (Figure 7, top panel), and energy dissipation is high. The north and middle channels of Hampton Inlet, however are more reflective in nature, and show a sea surface elevation-along-channel velocity phase of almost 90˚, and corresponds with low energy dissipation. The south channel of Hampton Inlet is similar in nature to New River Inlet, with large energy losses and phase changes in the M2 tide, however sea surface elevation-along-channel velocity phase is more reflective in nature. Further work is needed to determine the dynamics in this channel. The Piscataqua River-Great Bay system, NH lies somewhere in the middle and demonstrates both areas of progressive wave and high dissipation, as well as standing wave, low energy loss dynamics. The transition seems to occur in the Little Bay region, which connects the Great Bay to the Piscataqua River. Further observation and modeling studies are needed to determine the nature of this transition.

4.2 Time Series and Harmonic Growth

Upstream evolution of the pressure-velocity phase relationships at the M_2 tidal frequency is shown in the top panel of Figure 7. Both New River and Great Bay phase relationships show transition from a dominantly progressive wave motion at the mouth (with slack water occurring about 1.7-2.6 hours after high tide near the mouths) to a more standing wave motion (only 0.3 hours difference in the upper parts of the estuary). Conversely at Hampton, slack tides at the mouth occur about 0.2-0.3 hours after high tide, and progressively later as the tide propagates up the estuary (reaching about 1 hour delay far into the south channel).

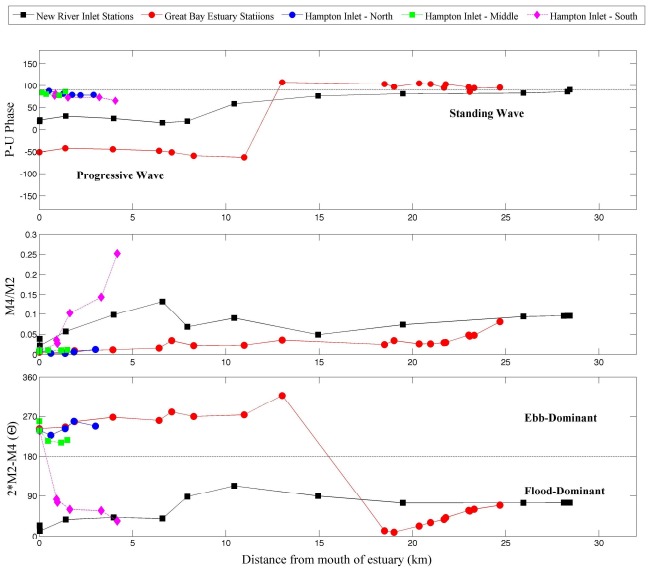

Figure 7: Relative energy decay and phase change in the M2 tidal signal for all of the model cases.

The ratio of the M_4 to M_2 amplitudes are a measure of the non-linear distortion of the tide (Friedrichs and Aubrey, 1988) and depends strongly

on the geometry and frictional features in the tidal channels and mudflats. Both New River Inlet and the south channel of Hampton Inlet show large ratios, and therefore large tidal distortion. In New River, within the first 7 km of the estuary exists the greatest growth of the M_4 overtide, corresponding to the greatest energy dissipation in the system. As before, similar dynamics are observed in the south channel of Hampton Inlet. Both systems show low harmonic phase differences and exhibit flood-dominant characteristics.

The growth of the M_4/M_2 ratio around Great Bay (~20 km in Figure 7) aligns with earlier observations of tidal asymmetry growing with distance into the estuary (shown in Figure 4). The corresponding phase difference shows a transition towards flood-dominance in the same region as the ratio, possibly due to geometry changes in the estuary. The Piscataqua River is a relatively deep channel with strong tidal currents, and transitioning to a large spatial region of mudflats in Great Bay, may dominate the tidal distortion in this case (Friedrichs and Aubrey, 1988).

5. Conclusion

Tidal energy dissipation was examined through tidal amplitude and phase changes as well as harmonic growth in three estuaries using a three-dimensional fully nonlinear hydrodynamic model. Nonlinear evolution of the tides was qualitatively examined with the spatial evolution of the skewness and asymmetry, and the growth of harmonic constituents. Previous hydrodynamic modeling and observational studies of tidal inlets show that that the nonlinear evolution of the tides is strongly dependent on the bottom boundary conditions (*e.g.*, MacMahan, et al., 2014).

Modeled tidal behavior in New River is calibrated with previous results based on force balance between pressure gradients and bottom drag and verified with observed elevation time series (MacMahon, 2014). Strong tidal dissipation is evident in the energy decay and phase change in the M_2 tidal component as a function of distance from the inlet, shown in Figure 6. The high ratio of the M_2/M_4 shown in Figure 7 tide also corresponds to higher energy losses than the other two estuaries. The M_2-M_4 phase difference suggests flood-dominance.

In the Piscataqua River/Great Bay Estuary, model bottom roughness (assumed constant over the domain) was calibrated with observations of surface elevation and current time series obtained throughout the estuary. The modeled behavior reproduces a highly dissipative progressive wave in the Piscataqua River with 45% tidal energy decay, and a standing wave low dissipative region in the Great Bay. This is similar to results shown in the literature (~52%, Swift and Brown, 1979) and observations. Future work is needed to determine the spatial variability of the bottom roughness in the model, and how that relates to the spatial variability in the energy dissipation.

Modeled tidal behavior in Hampton shows marked differences in tidal dissipation between channels, confirming previous estimates of limited energy loss in two channels (Ward and Irish, 2014), but with significant energy loss (> 80%) in the third Hampton channel, similar to New River Inlet. Strong spatial variation in the nonlinear evolution of the higher harmonics at Hampton reveals complex tidal shoaling within the shallow back-bay area. The differences in nonlinear tidal evolution between estuaries and channels are attributed to the integrated amount of energy dissipated along different path lengths of the various estuarine branches. Observed evolution of tidal dissipation, harmonic growth, and nonlinear statistics are also well modeled, indicating that the nonlinear evolution of the tides is well represented in COAWST.

Acknowledgements

We gratefully thank the many people involved in collecting bathymetric observations, including for New River Inlet Jesse McNinch of the USACE FRF, Jamie Macmahan, Naval Postgraduate School, and Ad Reniers, TUDelft. Kate Von Krusenstiern collected bathymetric datasets and provided grid development and modeling work for Hampton Harbor. Jim Irish provided guidance with the tidal analysis as well as

leading several instrument deployments. Computations were performed on Trillian, a Cray XE6m-200 supercomputer at UNH supported by NSF MRI program under grant PHY-1229408. This research was supported through grants from the ONR Littoral Geosciences and Optics Program, NOAA Office of Coast Survey, and UNH.

References

Aubrey, D., Speer, P.E. 1985. A study of Non-linear tidal propagation in shallow Inlet/Estuarine Systems. Part I : Observations. *Estuarine, Coastal and Shelf Science.* 21: 185-205.

Burkholder, J.M., M.A. Mallin, H.B. Glasgow, Jr., L.M. Larsen, M.R. McIver, G.C. Shank, N. Deamer-Melia, D.S. Briley, J. Springer, B.W. Touchette and E. K. Hannon. 1997. Impacts to a coastal river and estuary from rupture of a swine waste holding lagoon. *Journal of Environmental Quality*. 26:1451-1466.

Dronkers, J. 1986. Tidal Asymmetry and Estuarine Morphology. *Netherlands Journal of Sea Research*. 20 (2/3) :117-131.

Egbert, G.D., Erofeeva, S.Y., 2002. Efficient Inverse Modeling of Barotropic Ocean Tides. Journal of Atmospheric and Oceanic Technology. 19: 183-204.

Friedrichs, C., Aubrey, D., 1988. Non-linear tidal distortion in shallow well-mixed estuaries : a synthesis. *Estuarine, Coastal and Shelf Science.* 27: 521-545.

Haidvogel, D.B., Arango, H., Budgell, W.P., Cornuelle, B.D., Curchitser, E., Di Lorenzo, E., Fennel, K., Geyer, W.R., Hermann, A.J., Lanerolle, L., Levin, J., McWilliams, J.C., Miller, A.J., Moore, A.M., Powell, T.M., Shchepetkin, A.F., Sherwood, C.R., Signell, R.P., Warner, J.C., Wilkin, J., 2008. Ocean forecasting in terrain-following coordinates: formulation and skill assessment of the Regional Ocean Modeling System. *Journal of Computational Physics*. 227 : 3595–3624.

MacMahan, J., et al., 2014. Fortnightly tides and subtidal motions in a choked inlet. *Estuarine, Coastal and Shelf Science.* Volume 150, Part B: 325-331.

Mallin, M.A., Cahoon, L.B., McIver, M.R., Parsons, D.C., Shank, G.C., 1997. Nutrient limitation and eutrophication potential in the Cape Fear and New River estuaries. Report No. 313. Water Resources Research Institute of the Universityof North Carolina, Raleigh, North Carolina.

McKenna, L, 2013. Patterns of bedform migration and mean tidal currents in Hampton Harbor Inlet, New Hampshire, USA. *M.S. Thesis,* University of New Hampshire. 106 pp.

New Hampshire Estuaries Project. 2007. Hydrologic parameters for New Hampshire's estuaries. Prepared by P. Trowbridge, NHDES. Available at : http://www.nhep.unh.edu/resources/pdf/hydrologic_parameters_for nhep_07.pdf.

NOAA, 1999. Physical and hydrologic characteristics of coastal watersheds. Coastal Assessment and Data Synthesis (CA&DS) System. National Coastal Assessments Branch, Special Projects Office, National Ocean Service, National Oceanic and Atmospheric Administration. Silver Spring, MD.

Pawlowicz, R., Beardsley, B., and Lentz, S., 2002. Classical tidal harmonic analysis including error estimates in MATLAB using T_TIDE. *Computers and Geosciences*. 28: 929-937.

Shchepetkin, A.F., McWilliams, J.C., 2005. The Regional Oceanic Modeling System (ROMS): A split-explicit, free-surface, topography-following-coordinate oceanic model. *Ocean Modeling*. 9: 347–404

Short, F.T., The Ecology of the Great Bay Estuary, New Hampshire and Maine: An Estuarine Profile and Bibliography, NOAA-Coastal Ocean Program. Publ. 222 pp.

Speer, P.E., Aubrey, D., 1985. A study of Non-linear tidal propagation in shallow Inlet/Estuarine Systems. Part II: Theory. *Estuarine, Coastal and Shelf Science.* 21: 207-224.

Swift, R., and Brown, W., 1983. Distribution of Bottom Stress and Tidal Energy Dissipation in a Well-Mixed Estuary. *Estuarine Coastal and Shelf Science*. 17: 297-317.

Umlauf, B.H., Burchard, H. 2003. A generic length-scale equation for geophysical turbulence models. *Journal of Marine Research*. 61, 235-265.

Ward, L.G., Irish, J. D., 2014. Morphologic Changes of a Heavily Developed and Modified Back-Barrier System: Hampton-Seabrook Harbor, New Hampshire. *GSA Annual Meeting*. Vancouver, British Columbia, Canada, paper 340-3.

Warner, J.C., Sherwood, C., Arango, H., Signel, R. 2005. Performance of four turbulence closure models implemented using a generic length scale method. *Ocean Modeling*. 8, 81-113.

Warner, J.C., Defne, Z., Haas, K., Arango, H. 2013. A wetting and drying scheme for ROMS. *Computers & Geosciences.* 35, 54-61.

Warner, J. C., Armstrong, B., He, R., and Zambone, J. B., 2010. Development of a Coupled Ocean–Atmosphere–Wave–Sediment Transport (COAWST) Modeling System. *Ocean Modeling*. 35: 230-244.